Academic Journal of Science and Technology
ISSN: 2771-3032 | Vol. 5, No. 2, 2023

Design and Fabrication of Two-stage SQUID for Transition Edge Sensor

Yingyu Chen[1, 3, 4], Chaoqun Wang[1, 3, 4], Yuanxing Xu[2], Yue Zhao[1, 3, 4], Lihong Tang[1, 3], Bo Gao[1, 3, 4, a]

[1]Shanghai Institute of Microsystem and Information Technology, Chinese Academy of Sciences, Shanghai 200050, China
[2]Shanghai Institute of Optics and Fine Mechanics, Chinese Academy of Sciences, Shanghai 201800, China
[3]CAS Center for Excellence in Superconducting Electronics (CENSE), Shanghai 200050, China
[4]University of Chinese Academy of Sciences, Beijing 100049, China
[a]bo_f_gao@mail.sim.ac.cn

Abstract: The X-ray transition edge sensor (TES) modeled by calorimeter is extremely sensitive to temperature changes when operating at a voltage bias in the mK temperature region, and is widely used for the detection of particles and photons from submicron frequency to gamma rays. Superconducting quantum interference device (SQUID) is the key to TES current signal readout, we have designed a two-stage SQUID amplifier circuit. First-stage sensor SQUID uses first-grade gradiometer with high input mutual inductance about $176.2pH$, it increases the coupling sensitivity with the TES detector and has stronger resistance to external interference. Second-stage SQUID array(SSA) adopts 32 single SQUIDs in series, which has low magnetic flux noise and high magnification. We have verified the characteristics of this two-stage circuit and demonstrated that it has a lower magnetic flux noise.

Keywords: Translation Edge Sensors, SQUID, two-stage.

1. Introduction

In actual TES sensor signal readout, two-stage SQUID amplifiers composed of sensor SQUID and SSA in series have better readout performance and are widely used, the two-stage SQUID amplifier readout circuit designed by V.Foglietti was first proposed at CNR-IESS in Rome[1]. It consists of two cascaded SQUID parts, compared to single-stage SQUID direct readout, this cascade structure is more suitable for flux locking loop(FLL) operation, effectively improving the linear flux range in FLL mode[2]. The use of primary sensor SQUID increases the sensitivity of coupling to TES detectors, while providing stronger resistance to external interference, and requires lower performance requirements for room temperature circuits. The current signal coupled through the primary SQUID enters the current biased secondary SSA again, passing through the flux-voltage transfer coefficient V_Φ realize amplification[3].

Using a two-stage circuit not only improves the linear magnetic flux range and the ability to resist noise interference, but also greatly simplifies the readout circuit. Due to high stability and reducing the equivalent noise of the room temperature amplifier, there is no need for flux modulation technology or impedance matching between SQUID and the room temperature amplifier, greatly increasing the bandwidth of the circuit[4]. Similarly, the FLL feedback circuit is used to achieve the working point locking of the primary SQUID, and the secondary SQUID array is used to improve the large output voltage and voltage transfer coefficient V_Φ, while maintaining the linear magnetic flux range of the primary sensor SQUID[5]. In terms of readout noise, due to the sufficiently high gain of SSA, the flux noise of primary SQUIDs will be much greater than the flux noise of SSA[6]. Therefore, the output noise of the entire system is determined by the primary sensor SQUID and exceeds the noise of the room temperature preamplifier[7]. Therefore, designing a low noise first-stage sensor SQUID is the key to the signal readout of a TES detector, and its current noise should be less than the current noise of the TES. Currently, the current noise of the TES is about $90\text{pA}/\sqrt{Hz}$, and a good sensor SQUID has a magnetic flux noise at 4.2K below $1.0\mu\Phi_0/\sqrt{Hz}$ and with input coil mutual inductance M_{in} should be as large as possible to achieve high coupling while ensuring its equivalent current noise level is lower than the TES detector[8].

In the parameter design of the first-stage sensor SQUID, its input coil inductance L_{in} is typically at the nH level and the mutual inductance M_{in} between the input coil and the SQUID loop inductance is typically above 150 pH to ensure good coupling with TES detectors. At the same time, a low inductance double-loop first-grade gradiometer design or second-grade gradiometer design can reduce the magnetic flux noise of the first-stage SQUID[9]. For the second-stage SSA, a sufficient number of single SQUIDs are connected in series to ensure a large flux-voltage transfer coefficient V_Φ and lower magnetic flux noise.

2. First-stage Sensor SQUID Design and Fabrication

We have designed a first-grade gradiometer sensor SQUID，figure 1(a) and (b) show a schematic and an optical microscope picture of the sensor SQUID. The two octagonal washers are sensor loop inductance, coil about 5 turns indicates the input coil, the mutual inductance M_{in} between it and washers is $176.2pH$. The one turn coil is feedback coil, and the mutual inductance M_f is about $45.8pH$. The input coil is used to couple the TES current signal, while the feedback coil is used to provide a working bias current to the sensor SQUID. In this design, the diameter of the washer hole of the sensor SQUID is $22um$, and the width of the washer is $28um$, and the inductance of SQUID washer loop L_S is about 136.9pH. Shunt resistor R_s in parallel with Josephson junction is 8Ω, in practical fabrication, Ti/Pd thin films are

used as shunt resistor R_s. In order to cool the shunt resistor R_s, we have designed a cooling resistor called cooling fin, which can effectively reduce the thermal noise caused by the heating of the shunt resistor[10]. The Josephson junction area is approximately $2.8um \times 2.8um$, and the critical current density $J_c = 100A/cm^2$ in the fabrication, so the critical current I_c is about $7.9\,uA$. This result in a screening parameter $\beta_L = 2L_S I_c/\Phi_0 \approx 1.04$ and hysteresis parameter $\beta_C = 2\pi R^2 C I_c/\Phi_0 \approx 0.5$.

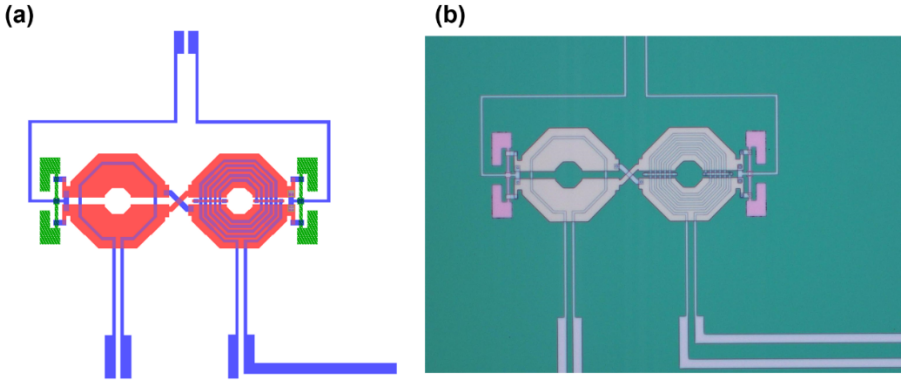

Figure 1. (a) Schematic; (b) optical microscope picture of the sensor SQUID. Coil with large turns indicates an input coil, while a smaller number indicates a feedback coil.

When the first-stage sensor SQUID operates, it typically uses voltage bias to detect the TES signal and output a varying current. In practice, a bias resistor about 0.5 Ω is used to form a voltage bias in parallel with SQUID. When a linearly varying magnetic flux current is applied, the SQUID output is I-Φ characteristic curve, the change of SQUID output current with magnetic flux[11]. I-Φ curve is a periodic sinusoidal curve, whose period also depends on the mutual inductance of the input coil. The maximum current modulation depth of the sensor SQUID I - Φ curve is about 6.3uA, and the corresponding maximum slope on the curve, that is, the current-flux transfer coefficient I_Φ, is $20uA/\Phi_0$.

In 1981, Rowell et al. discovered that depositing a very thin aluminum film (typically 2-4nm) on a clean Nb surface and adding an aluminum oxide layer can prepare high-quality Josephson junctions on the basis of Nb thin films, named $Nb/Al-AlO_x/Nb$, three-layer thin film fabrication[12]. The fabrication used in this paper is the Nb06 fabrication of the Chinese Academy of Sciences Shanghai Institute of Microsystems. First, Ti/Pd thin film was sputtered on a 4-inch wafer as a metal junction parallel resistance layer, followed by the addition of an insulation layer and wiring layer. Then sputtering growth of $Nb/Al-AlO_x/Nb$ thin films on the insulation layer, and synchronous photolithography and RIE etching are performed on the top and bottom of the three-layer film. Finally, an insulating layer and wiring layer are added to form a complete SQUID fabricated process[13].

3. 32-SQUID series arrays

Using the design method and processes similar to sensor SQUID, we designed and obtained 32-SQUID series arrays(32-SSA), unlike the primary sensor SQUID, SSA uses current bias. In this case, we can obtain the output characteristic curve and noise performance of SSA.

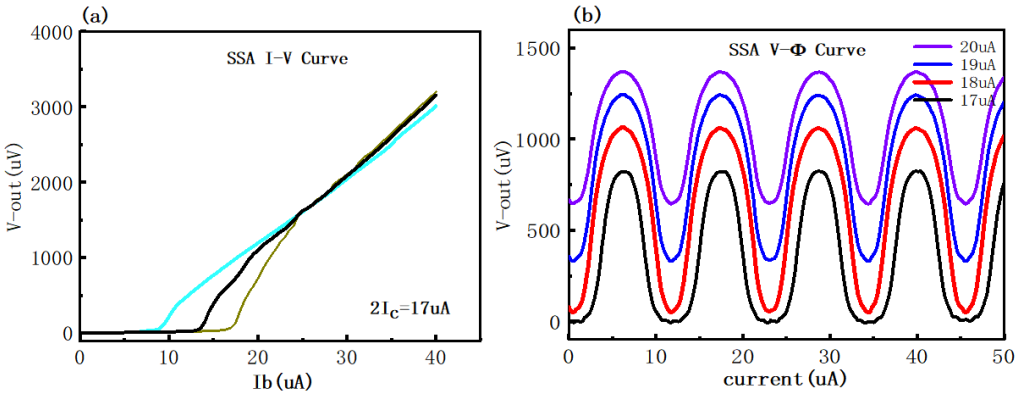

Figure 2. (a) SSA I-V curve; (b) SSA V-Φ curve

The I-V curve of SSA is usually composed of three characteristic curves, as shown in figure 2(a), the green curve indicates that when the magnetic flux added to the loop by the input coil is $n\Phi_0$, the relationship between the corresponding output voltage and the bias current. The bias current corresponding to the transition of the curve from the superconducting state to the normal state is the maximum critical current of SSA, which is about $17uA$. The blue and black curves indicate the I-V curve of the SSA when the magnetic flux added to the loop by the input coil are $\Phi_0/2$ and $\Phi_0/4$. Figure 2(b) shows the V-Φ curves corresponding to different I_b under current bias, when I_b =$18uA$, the V-Φ curve has the maximum voltage modulation depth $V_{pp} = 1050uV$, and the corresponding flux-voltage transfer coefficient V_Φ at the maximum slope of the curve is $3.5mV/\Phi_0$.

The working point of the SSA corresponding to the maximum slope of the V-Φ curve, at the working point, we measured the noise performance of the SSA. Figure 3(a) shows that the SSA does not pass through the FLL loop, but directly connects the output of the SSA to the audio analyzer. After obtaining the voltage signal and undergoing FFT processing, using the conversion coefficient $V_\Phi = 3.5mV/\Phi_0$, the magnetic flux noise spectral density at the white noise section at $200Hz$ is approximately $0.51u\Phi_0/\sqrt{Hz}$. Using input coil mutual inductance $M_{in} = \Phi_0/11.6uA = 176.2pH$, we can obtain a corresponding current noise spectral density of $6.2pA/\sqrt{Hz}$ in open loop amplification model.

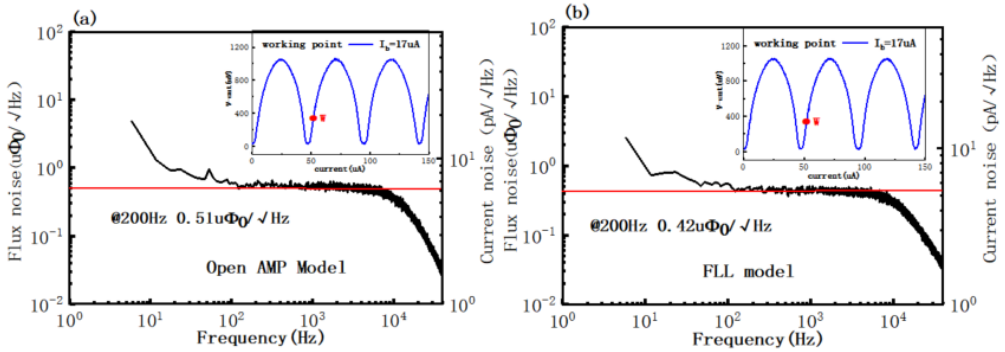

Figure 3. (a) Noise performance in open loop amplification model; (b) Noise performance in FLL model

Similarly, when using a FLL feedback loop for closed-loop measurement, the SSA's working point should be selected at the maximum slope to minimize the equivalent noise of the room temperature amplifier. Unlike open loop, when closed loop, the SSA's operating point will be locked by the FLL feedback loop. At this point, the flux-voltage transfer coefficient becomes $V_F = R_f/M_f$, which $R_f = 100K\Omega$ is the FLL feedback loop resistance. In FLL model, the magnetic flux noise spectral density at the white noise section at $200Hz$ is approximately $0.42\ u\Phi_0/\sqrt{Hz}$ and the current noise spectral density is $5.4pA/\sqrt{Hz}$.

4. Two-stage SQUID circuit

The basic components of a two-stage circuit are sensor SQUID and SQUID series array (SSA)[14], using the two devices mentioned above, we successfully built a two-stage circuit and measured its output characteristic curve and noise performance. Figure 4 shows the total output of the two-stage related to the selection of the secondary SSA working point, when the working point of the secondary SSA is in the linear range, the two-stage output has the maximum voltage modulation depth $V_{pp,t}$, and the entire system has the maximum flux voltage conversion coefficient $V_{\Phi,t}$.

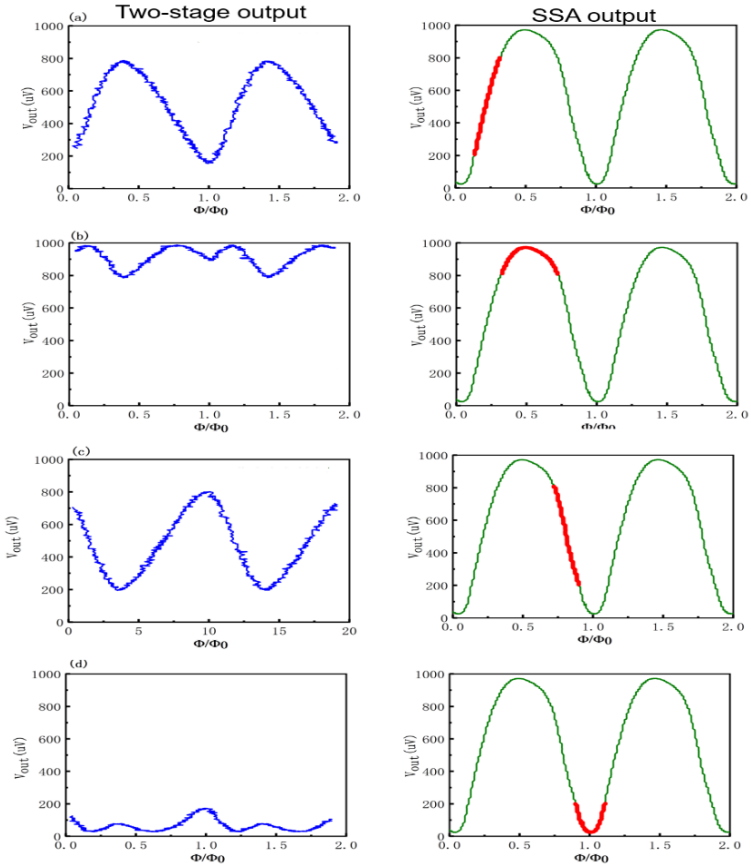

Figure 4. When the selection of the secondary SSA working point is different, the total output of the two-stage will change

Similarly, the noise performance of the two-stage circuit composed of the above devices is tested using the audio analyzer. In the open loop amplification mode, figure 5(a) shows the magnetic flux noise spectral density at the white noise section at $200Hz$ is $1.15u\Phi_0/\sqrt{Hz}$ and the current noise spectral density of $12.4pA/\sqrt{Hz}$. Next, the noise of the two-stage circuit in the FLL model is measured, as shown in figure 5(b), its working point remains consistent with that in the open loop model. We obtained the magnetic flux noise spectral density at the white noise section at $200\,Hz$ is approximately $0.98u\Phi_0/\sqrt{Hz}$ and the current noise spectral density is $11.3pA/\sqrt{Hz}$.

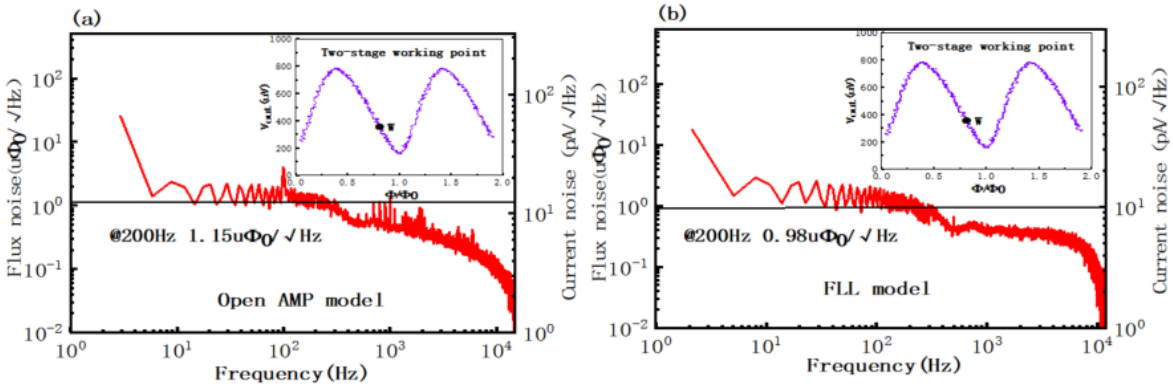

Figure 5. (a) Noise performance in open loop amplification model of two-stage; (b) Noise performance in FLL model of two-stage

5. Conclusion

This manuscript focuses on the research of two-stage SQUID amplification circuit for TES detector readout. We have designed and fabricated first-stage sensor SQUID and second-stage SQUID series array devices, and characterized their performance. First-stage sensor SQUID has a large input mutual inductance $M_{in} = \Phi_0/11.6uA = 176.2pH$, and can achieve good coupling with TES device. Second-stage SQUID series array consists of 32 SQUIDs in series, so compared to single SQUID, the SSA has a higher output voltage $V_{pp} = 1050uV$ and a larger flux-voltage transfer coefficient $V_\Phi = 3.5mV/\Phi_0$. Therefore, the magnetic flux noise of the SSA is as low as $0.42u\Phi_0/\sqrt{Hz}$. Finally, we measured the two-stage circuit and obtain its output characteristic curve, when the working point of the secondary SSA is in the linear range, the two-stage output has the maximum voltage modulation depth $V_{pp,t} = 600uV$. According to the test results, the magnetic flux noise of the device in the open loop mode is slightly greater than that in the FLL mode. The magnetic flux noise of the two- stage in FLL mode is as low as $0.98u\Phi_0/\sqrt{Hz}$, and the current noise spectral density is as low as $11.3pA/\sqrt{Hz}$. The current noise spectral density of the two-stage is much lower than the current noise spectral density of the TES, which can be well applied to the readout of TES.

References

[1] FOGLIETTI V, GIANNINI M E, PETROCCO G. A double DC-SQUID device for flux locked loop operation [J]. IEEE Transactions on Magnetics, 1991, 27(2): 2989-92.

[2] WELTY R P, MARTINIS J M. Two-stage integrated SQUID amplifier with series array output [J]. IEEE Transactions on Applied Superconductivity, 1993, 3(1): 2605-8.

[3] JAMES C, KENT I, ERICH G, et al. Superconducting Multiplexer for Arrays of Transition Edge Sensors [J]. 1999.

[4] CANTOR R, LEE L, MATLASHOV A N, et al. A low-noise, two-stage DC SQUID amplifier with high bandwidth and dynamic range [J]. Applied Superconductivity, IEEE Transactions on, 1997, 7: 3033-6.

[5] DRUNG D, CANTOR R, PETERS M, et al. Low-noise high-speed dc superconducting quantum interference device magnetometer with simplified feedback electronics [J]. 1990, 57: 406-8.

[6] TESCHE C D, CLARKE J. dc SQUID: Noise and optimization [J]. Journal of Low Temperature Physics, 1977, 29(3): 301-31.

[7] DRUNG D. Introduction to Nb-Based SQUID Sensors, F, 2016 [C].

[8] WAKEHAM N A, ADAMS J S, BANDLER S R, et al. High-Frequency Noise Peaks in Mo/Au Superconducting Transition-Edge Sensor Microcalorimeters [J]. Journal of Low Temperature Physics, 2020, 200(5): 192-9.

[9] TESCHE C D. Analysis of a double-loop dc SQUID [J]. Journal of Low Temperature Physics, 1982, 47(5): 385-410.

[10] FOGLIETTI V, GALLAGHER W J, KETCHEN M B, et al. Performance of dc SQUIDs with resistively shunted inductance [J]. 1989, 55: 1451-3.

[11] POLUSHKIN V, GLOWACKA D, HART R, et al. Cross-Correlated Dynamic Resistance of a Direct Current Superconducting Quantum Interference Device [J]. Journal of Low Temperature Physics, 2000, 118(1): 105-11.

[12] KROGER H, SMITH L N, JILLIE D W J A P L. Selective niobium anodization process for fabricating Josephson tunnel junctions [J]. 1981, 39: 280-2.

[13] ZHANG X, ZHANG G, YING L, et al. Fabrication and measurement of Nb-based SQUID magnetometer [J]. Physica C: Superconductivity and its Applications, 2018, 548: 1-4.

[14] KEMPF S, FERRING A, FLEISCHMANN A, et al. Direct-current superconducting quantum interference devices for the readout of metallic magnetic calorimeters [J]. 2015, 28.